

Superconductivity and antiferromagnetism in heavy-electron systems

Rikio Konno

Institute for Solid State Physics, University of Tokyo, Tokyo, Roppongi 106, Japan

Kazuo Ueda

Institute of Material Science, University of Tsukuba, Tsukuba 305, Japan

(Received 3 January 1989)

Superconductivity and antiferromagnetism in heavy-electron systems are investigated from a general point of view. First we classify superconducting states in a simple cubic lattice, a body-centered tetragonal lattice, and a hexagonal close-packed lattice, having URu_2Si_2 and UPt_3 in mind. For that purpose we take an approach to treat the effective couplings in real space. The approach is convenient to discuss the relation between the nature of fluctuations in the system and the superconducting states. When we assume that the antiferromagnetic fluctuations reported by neutron experiments are dominant, the most promising are some of the anisotropic singlet states and there remains the possibility for some triplet states too. Then we discuss the coupling between the two order parameters based on a Ginzburg-Landau theory. We derive a general expression of the coupling term. It is pointed out that the coupling constant can be large in heavy-electron systems. The general trend of the coexistence of the superconductivity and antiferromagnetism is discussed, and it is shown that the anisotropic states are generally more favorable to the coexistence than the conventional isotropic singlet. Experimental data of URu_2Si_2 and UPt_3 are analyzed by the Ginzburg-Landau theory. According to the analysis URu_2Si_2 has a small coupling constant and a large condensation energy of the antiferromagnetism. On the other hand, UPt_3 has a large coupling constant and a small condensation energy. It means that the specific-heat anomaly at T_N should be small in UPt_3 and its superconductivity is easily destroyed when a large moment is formed.

I. INTRODUCTION

In recent years intensive studies have been made on a new class of intermetallic compounds.^{1,2} In this class of materials, the effective mass determined by the T -linear term of the electronic specific heat ranges from several hundreds to a thousand times bigger than the bare electron mass, hence the name of heavy-electron (fermion) systems. The heavy mass originates from strong interaction among electrons. Therefore the first central question is why the heavy electron states are stabilized instead of some magnetic ordering. It was a real surprise when the superconductivity was discovered in some cerium and uranium compounds which had very large γ values, CeCu_2Si_2 ,³ URu_2Si_2 ,⁴ and UPt_3 .⁵ Concerning the superconductivity, a central issue is whether the superconducting state is an ordinary one or an unconventional one. Although there are many experimental indications to support the unconventional one, decisive experiments have not appeared yet.

The discovery of two transitions in URu_2Si_2 (Refs. 6–8) was the beginning of a more subtle question of interplay between magnetism and the heavy-electron state, although the effective mass of URu_2Si_2 is not so heavy. The neutron scattering experiments by Broholm *et al.*⁹ demonstrated that the upper transition, where specific heat shows a typical λ -type anomaly, is really to an antiferromagnetic state, $T_N=17.5$ K, and that below the second transition, $T_c=1.5$ K, superconductivity coexists with the antiferromagnetism. They reported unusually

small ordered moment $(0.03\pm 0.01)\mu_B$.

The first suggestion of the presence of magnetic ordering in UPt_3 came from muon-spin rotation (μSR) experiments.¹⁰ Neutron scattering experiments by Aeppli *et al.*¹¹ reported the coexistence of superconductivity and antiferromagnetism. According to their results, the Néel temperature is $T_N=5$ K and the magnitude of the ordered moment is small, $(0.02\pm 0.01)\mu_B$, and it stops to grow and stays constant below $T_c=0.5$ K. A mystery of UPt_3 is that no anomaly at T_N is observed by other experimental methods, especially in specific heat.

An indication of magnetic anomaly in CeCu_2Si_2 also came from μSR experiments. Uemura *et al.*¹² reported that $\text{CeCu}_{2.1}\text{Si}_2$ with $T_c=0.7$ K undergoes a spin-glass transition or a spin-density-wave (SDW) transition around 0.8 K. Very recently nuclear-magnetic-resonance (NMR) studies by Nakamura *et al.*¹³ found that a superconducting sample of $\text{CeCu}_{2.02}\text{Si}_2$ with $T_c=0.72$ K shows an SDW transition below 0.6 K in external magnetic field.

These examples show that the coexistence of superconductivity and antiferromagnetism in heavy-electron systems is not an exceptional case but rather a common phenomenon. A well-known example of the coexistence of magnetism and superconductivity is that of the magnetic superconductors. One of the new features here is that the same f electrons are responsible for both the antiferromagnetism and the superconductivity. Another interesting point is the smallness of the ordered moment. In the present paper we will not address the question of

microscopic origin of the small moment but use it as a fact to treat the problem of the coexistence. The smallness of the moment allows us to use Ginzburg-Landau expansion not only for the superconducting order parameter but also for the order parameter of the antiferromagnetism.

The organization of the present paper is the following. In Sec. II we discuss irreducible representations of the superconducting order parameter. We use an approach in real space. One of the advantages of the approach is that it is quite easy to have an idea about the relation between the nature of fluctuations which mediate the superconducting couplings and possible superconducting states. In Sec. III we develop a general theory of coupling between the superconductivity and the antiferromagnetism. There we will discuss the general trend of the coexistence phenomena among various possible superconducting states and estimate the magnitude of the coupling constant. In Sec. IV we will make an analysis of experimental data of URu₂Si₂ and UPt₃ based on the Ginzburg-Landau free energy. We will conclude the paper by summary and discussions in the Sec. V. A part of the present work has been reported elsewhere.¹⁴

II. ANISOTROPIC SUPERCONDUCTIVITY

In the heavy-fermion superconductors, it is well known¹ that various physical quantities such as specific heat, the NMR relaxation rate, and the coefficient of ultrasonic attenuation show power-law behavior instead of the exponential temperature dependence predicted by the BCS theory. Such power-law behavior come from low-energy excitations existing in the superconducting state, suggesting some anisotropic state. A *p*-wave state was proposed for UBe₁₃ based on the *T*³ behavior of specific heat¹⁵ and also by the analogy with ³He.¹⁶ Ohkawa and Fukuyama proposed an anisotropic *s*-wave state.¹⁷ It was also pointed out that the antiferromagnetic fluctuations are favorable to a *d*-wave state.^{18,19} Classification of the anisotropic states were done by Volovik and Gor'kov,²⁰ Ueda and Rice,²¹ and Blount.²² In these classifications basis functions of spherical harmonics in *k* space are used. In the present paper we will use an approach in real space. One of the advantages of the present approach is that it is easy to see the relation between the superconducting states and the nature of charge or spin fluctuations which mediate the pairing interactions. Another advantage is that the basis functions are compatible with the translation of the lattice.²³ As specific examples, we take a simple cubic (sc) lattice, a body-centered tetragonal (bct) lattice, and a hexagonal close-packed (hcp) lattice. The bct lattice is appropriate for URu₂Si₂ and CeCu₂Si₂ and for UPt₃ the hcp lattice is appropriate.

A. Simple cubic lattice

As a guide to more complicated systems of the bct and the hcp, we use a simple cubic lattice and consider orbitally nondegenerate case. We take into account residual interactions between quasiparticles in real space. The first term is the on-site interaction

$$V_0 n_{i\uparrow} n_{i\downarrow}. \quad (2.1)$$

For the nearest-neighbor pairs, there are couplings between charge densities and also between spin densities,

$$V_1 n_{i+\delta} n_i, \quad (2.2)$$

$$J_1 \mathbf{s}_{i+\delta} \cdot \mathbf{s}_i. \quad (2.3)$$

Note that V_0 is different from the bare on-site Coulomb interaction but related to the Landau parameter F_0^s . We expect repulsive V_0 for heavy-electron materials even if we include electron-phonon couplings.²⁴ We can proceed to the next-nearest-neighbor pairs and so on. But the nearest-neighbor couplings are sufficient to understand qualitative natures.

In general, from given couplings, pairing interactions for Cooper pairs are obtained in the form of

$$\frac{1}{N} \sum_{\Gamma_s, \gamma_{\Gamma_s}} V_{\Gamma_s} \psi_{\gamma_{\Gamma_s}}^{(0)\dagger} \psi_{\gamma_{\Gamma_s}}^{(0)} + \frac{1}{N} \sum_{\Gamma_t, \gamma_{\Gamma_t}} \sum_{j=1}^3 V_{\Gamma_t} \psi_{\gamma_{\Gamma_t}}^{(j)\dagger} \psi_{\gamma_{\Gamma_t}}^{(j)}, \quad (2.4)$$

where the first term is for singlet pairings and the second term for triplet pairings. Γ denote irreducible representations and γ_{Γ} stand for their basis functions. V_{Γ} is the coupling constant for the irreducible representation Γ . It should be noted that once the couplings are given the irreducible representations are determined. $\psi_{\gamma_{\Gamma}}^{(0)}$ is a field operator for singlet Cooper pairs $\psi_{\gamma_{\Gamma}}^{(j)}$ are field operators ($j=1,2,3$) for triplet Cooper pairs. The field operators are defined by annihilation operators $a_{k\alpha}$ as

$$\psi_{\gamma_{\Gamma_s}}^{(0)} = -\frac{1}{2} \sum_k \sum_{\alpha, \beta} \phi_{\gamma_{\Gamma_s}}(k) a_{-k\alpha} (\sigma_2 \sigma_0^i)_{\alpha\beta} a_{k\beta}, \quad (2.5)$$

$$\psi_{\gamma_{\Gamma_t}}^{(j)} = -\frac{1}{2} \sum_k \sum_{\alpha, \beta} \phi_{\gamma_{\Gamma_t}}(k) a_{-k\alpha} (\sigma_2 \sigma_j^i)_{\alpha\beta} a_{k\beta}, \quad (2.6)$$

where σ_j ($j=1,2,3$) are Pauli matrices and $\sigma_0 = \sigma_1 \sigma_2 \sigma_3$. Internal wave function or the form factor of the Cooper pairs is represented by a basis function $\phi_{\gamma_{\Gamma}}(k)$.

For the gap matrix $\Delta(k)$, we use the standard four-vector notation

$$\begin{aligned} \Delta(k) &= i \sum_{i=0}^3 (\sigma_i \sigma_2) d_i(k) \\ &= \begin{bmatrix} -d_1(k) + id_2(k) & id_0(k) + d_3(k) \\ -id_0(k) + d_3(k) & d_1(k) + id_2(k) \end{bmatrix}. \end{aligned} \quad (2.7)$$

The order parameter $d_i(k)$ is given by the average of the field operators

$$d_i(k) = \frac{1}{N} \sum_{\Gamma} \sum_{\gamma_{\Gamma}} V_{\Gamma} \langle \psi_{\gamma_{\Gamma}}^{(i)} \rangle \phi_{\gamma_{\Gamma}}(k). \quad (2.8)$$

In the present case of the simple cubic lattice with up to the nearest-neighbor couplings, Eqs. (2.1)–(2.3), we have two one-dimensional representations, Γ_1^+ , one two-dimensional representation, Γ_3^+ , and one three-dimensional representation, Γ_4^- . The parity of the first three irreducible representations is even (singlet pairings)

TABLE I. Irreducible representations of Cooper pairs in the simple cubic lattice with the nearest-neighbor couplings.

Γ	V_Γ	γ_Γ	ϕ_{γ_Γ}
Γ_1^+	V_0		1
Γ_1^+	$V_1 - \frac{3}{4}J_1$		$(\frac{2}{3})^{1/2}(\cos k_1 + \cos k_2 + \cos k_3)$
Γ_3^+	$V_1 - \frac{3}{4}J_1$	u	$\frac{1}{\sqrt{3}}(\cos k_1 + \cos k_2 - 2 \cos k_3)$
		v	$\cos k_1 - \cos k_2$
Γ_4^-	$V_1 + \frac{1}{4}J_1$	x	$\sqrt{2} \sin k_1$
		y	$\sqrt{2} \sin k_2$
		z	$\sqrt{2} \sin k_3$

and the last spin-orbit coupling). The coupling constants and the basis functions are tabulated in Table I. We use the lattice constant as the unit of length, $a=1$, and $\mathbf{k}=(k_1, k_2, k_3)$.

The first of the two Γ_1^+ representations is the conventional singlet s -wave state. The second Γ_1^+ is the extended s wave, and the Γ_3^+ representation corresponds to the d wave ($d\gamma$) one, and the Γ_4^- representation to the p wave one. In general, when we include higher-order couplings, the two representations of Γ_1^+ mix. When antiferromagnetic fluctuations are dominant, J_1 is positive and we expect either the extended s -wave or d -wave state as the most stable state. If the spin-orbit coupling is strong we have to include it to discuss the Γ_4^- representation, and this has been done in Refs. 20–22. The present form of the basis functions is compatible with the translation of the lattice. We would like to point out that $\phi_{\gamma_\Gamma}(k)$ for the second Γ_1^+ , Γ_3^+ , and Γ_4^- change their sign when k is shifted by the antiferromagnetic wave vector $Q=(\pi, \pi, \pi)$.²³

B. Body-centered tetragonal lattice

URu_2Si_2 and CeCu_2Si_2 have tetragonal ThCr_2Si_2 structures and there are two uranium or cerium atoms in a unit cell, forming a body-centered tetragonal lattice (Fig. 1). The effective couplings start from the on-site interaction

$$V_0 n_{i\uparrow} n_{i\downarrow}. \quad (2.9)$$

For the nearest-neighbor pairs in the basal plane, there are couplings between charge densities

$$V_p n_{i+\delta} n_i, \quad (2.10)$$

as well as between spin densities

$$J_p \mathbf{s}_{i+\delta} \cdot \mathbf{s}_i. \quad (2.11)$$

For the next-nearest-neighbor pairs between the body corners and the body centers, we also consider couplings between charge densities

$$V_c n_{i+\tau} n_i \quad (2.12)$$

and between spin densities

$$J_c \mathbf{s}_{i+\tau} \cdot \mathbf{s}_i. \quad (2.13)$$

We can proceed further if it is necessary.

From the given couplings, Eqs. (2.9)–(2.13), basis functions of the irreducible representations are obtained in the form of Eq. (2.4). This differs from the simple cubic case in that we need two kinds of operators, $a_{1k\alpha}$ and $a_{2k\alpha}$, since there are two atomic orbitals in the unit cell. $a_{1k\alpha}$ is the annihilation operator for electronic state which has its amplitude on the corner positions and $a_{2k\alpha}$ on the body-center positions. Accordingly, expressions for the fields operators for the Cooper pairs are modified as

$$\psi_{\gamma_{\Gamma_s}}^{(0)} = -\frac{1}{2} \sum_k \sum_{\alpha, \beta, n, m} \phi_{\gamma_{\Gamma_s}}^{nm}(k) a_{n-k\alpha} (\sigma_2 \sigma_0^i)_{\alpha\beta} a_{mk\beta}, \quad (2.14)$$

$$\psi_{\gamma_{\Gamma_t}}^{(j)} = -\frac{1}{2} \sum_k \sum_{\alpha, \beta, n, m} \phi_{\gamma_{\Gamma_t}}^{nm}(k) a_{n-k\alpha} (\sigma_2 \sigma_j^i)_{\alpha\beta} a_{mk\beta}. \quad (2.15)$$

The difference between the singlet and the triplet is the transformation property under the parity operation:

$$\phi_{\gamma_{\Gamma_s}}^{11}(k) = \phi_{\gamma_{\Gamma_s}}^{11}(-k), \quad \phi_{\gamma_{\Gamma_s}}^{22}(k) = \phi_{\gamma_{\Gamma_s}}^{22}(-k), \quad (2.16)$$

$$\phi_{\gamma_{\Gamma_s}}^{12}(k) = \phi_{\gamma_{\Gamma_s}}^{21}(-k),$$

$$\phi_{\gamma_{\Gamma_t}}^{11}(k) = -\phi_{\gamma_{\Gamma_t}}^{11}(-k), \quad \phi_{\gamma_{\Gamma_t}}^{22}(k) = -\phi_{\gamma_{\Gamma_t}}^{22}(-k), \quad (2.17)$$

$$\phi_{\gamma_{\Gamma_t}}^{12}(k) = -\phi_{\gamma_{\Gamma_t}}^{21}(-k).$$

Irreducible representations of singlet pairings are tabulated in Table II and those of triplet pairings are in Table III. The bct lattice is also a bipartite one. Therefore the basis functions originating from pairings connecting the two sublattices, the last six irreducible representations in

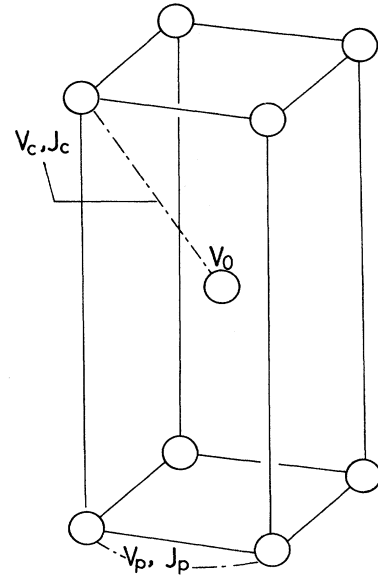


FIG. 1. Crystal structure of U atoms in URu_2Si_2 . V_0 is the on-site coupling constant, V_p and V_c are the coupling constants between the nearest-neighbor charge densities, and J_p and J_c are the coupling constants between the nearest-neighbor spin densities.

TABLE II. Irreducible representations of singlet Cooper pairs in the body-centered tetragonal lattice with the nearest-neighbor couplings.

Γ	V_Γ	γ	$\phi^{11}(k)$	$\phi^{12}(k)=\phi^{21}(-k)$	$\phi^{22}(k)$	
Γ_1^+	V_0		$\frac{1}{\sqrt{2}}$		$\frac{1}{\sqrt{2}}$	
Γ_1^+	V_0		$\frac{1}{\sqrt{2}}$		$-\frac{1}{\sqrt{2}}$	*
Γ_1^+	$V_p - \frac{3}{4}J_p$		$\frac{1}{\sqrt{2}}(\cos k_1 a + \cos k_2 a)$		$\frac{1}{\sqrt{2}}(\cos k_1 a + \cos k_2 a)$	
Γ_1^+	$V_p - \frac{3}{4}J_p$		$\frac{1}{\sqrt{2}}(\cos k_1 a + \cos k_2 a)$		$-\frac{1}{\sqrt{2}}(\cos k_1 a + \cos k_2 a)$	*
Γ_3^+	$V_p - \frac{3}{4}J_p$		$\frac{1}{\sqrt{2}}(\cos k_1 a - \cos k_2 a)$		$\frac{1}{\sqrt{2}}(\cos k_1 a - \cos k_2 a)$	
Γ_3^+	$V_p - \frac{3}{4}J_p$		$\frac{1}{\sqrt{2}}(\cos k_1 a - \cos k_2 a)$		$-\frac{1}{\sqrt{2}}(\cos k_1 a - \cos k_2 a)$	*
Γ_1^+	$V_c - \frac{3}{4}J_c$			$2 \cos \frac{1}{2}k_1 a \cos \frac{1}{2}k_2 a \cos \frac{1}{2}k_3 c$		
Γ_4^+	$V_c - \frac{3}{4}J_c$			$2 \sin \frac{1}{2}k_1 a \sin \frac{1}{2}k_2 a \cos \frac{1}{2}k_3 c$		
Γ_5^+	$V_c - \frac{3}{4}J_c$	$-zx$		$-\sin \frac{1}{2}k_1 a \cos \frac{1}{2}k_2 a \sin \frac{1}{2}k_3 c$		
		zy		$\cos \frac{1}{2}k_1 a \sin \frac{1}{2}k_2 a \sin \frac{1}{2}k_3 c$		
$\Gamma_2^-, \Gamma_3^-, \Gamma_5^-$	$V_c - \frac{3}{4}J_c$			see Table III		*

Table II or Table III, change their sign by the shift of \mathbf{k} to $\mathbf{k} + \mathbf{Q}$. On the other hand, basis functions due to pairings within a sublattice do not change their sign by the shift. Now we diagonalize the single-particle Hamiltonian, which generally has the following form:

$$H = \sum_k \sum_\alpha (a_{1k\alpha}^\dagger, a_{2k\alpha}^\dagger) \begin{bmatrix} \epsilon_0(k) & \epsilon_1(k) \\ \epsilon_1^*(k) & \epsilon_0(k) \end{bmatrix} \begin{bmatrix} a_{1k\alpha} \\ a_{2k\alpha} \end{bmatrix}. \quad (2.18)$$

In the bct lattice, each atomic position has the symmetry of the point group, D_{4h} (the space group is symmorphic). Therefore $\epsilon_1(k)$ is real, and the single-particle Hamiltonian is diagonalized simply by the unitary transformation

$$\begin{bmatrix} c_{1k\alpha} \\ c_{2k\alpha} \end{bmatrix} = \frac{1}{\sqrt{2}} \begin{bmatrix} 1 & \text{sgn}(\epsilon_1) \\ -\text{sgn}(\epsilon_1) & 1 \end{bmatrix} \begin{bmatrix} a_{1k\alpha} \\ a_{2k\alpha} \end{bmatrix}, \quad (2.19)$$

where $c_{1k\alpha}$ ($c_{2k\alpha}$) is the annihilation operator for the upper (lower) hybridized band, whose dispersion is $\epsilon_0(k) \pm |\epsilon_1(k)|$. When we take into account pairings within the same bands, which is a reasonable approxima-

tion, irreducible representations marked by * in the last column of the tables vanish and the same basis functions remain valid in the new representation for the other irreducible representations without *. Then the singlet (even parity) and triplet (odd parity) can be distinguished by the parity.

To see nature of the couplings, Eqs. (2.9)–(2.13), we make use of the Fourier transform. Since there are two atoms in the unit cell, there are two components, ρ_{1q} and ρ_{2q} , for the charge densities

$$\rho_{nq} = \sum_k \sum_\alpha a_{nk+q\alpha}^\dagger a_{nk\alpha}. \quad (2.20)$$

ρ_{1q} has its amplitude on the corner positions, while ρ_{2q} has its amplitude on the center positions. Similarly, the spin densities also have two components

$$s_{nq}^j = \frac{1}{2} \sum_k \sum_{\alpha, \beta} a_{nk+q\alpha}^\dagger (\sigma_j)_{\alpha\beta} a_{nk\alpha}. \quad (2.21)$$

The couplings between the charge densities are of the form

TABLE III. Irreducible representations of triplet Cooper pairs in the body-centered tetragonal lattice with the nearest-neighbor couplings.

Γ	V_Γ	γ	$\phi^{11}(k)$	$\phi^{12}(k)=-\phi^{21}(-k)$	$\phi^{22}(k)$	
Γ_5^-	$V_p + \frac{1}{4}J_p$	x	$\sin k_1 a$		$\sin k_1 a$	
		y	$\sin k_2 a$		$\sin k_2 a$	
Γ_5^-	$V_p + \frac{1}{4}J_p$	x	$\sin k_1 a$		$-\sin k_1 a$	*
		y	$\sin k_2 a$		$-\sin k_2 a$	*
Γ_2^-	$V_c + \frac{1}{4}J_c$			$2 \cos \frac{1}{2}k_1 a \cos \frac{1}{2}k_2 a \sin \frac{1}{2}k_3 c$		
Γ_3^-	$V_c + \frac{1}{4}J_c$			$2 \sin \frac{1}{2}k_1 a \sin \frac{1}{2}k_2 a \sin \frac{1}{2}k_3 c$		
Γ_5^-	$V_c + \frac{1}{4}J_c$	x		$2 \sin \frac{1}{2}k_1 a \cos \frac{1}{2}k_2 a \cos \frac{1}{2}k_3 c$		
		y		$2 \cos \frac{1}{2}k_1 a \sin \frac{1}{2}k_2 a \cos \frac{1}{2}k_3 c$		
$\Gamma_1^+, \Gamma_4^+, \Gamma_5^+$	$V_c - \frac{1}{4}J_c$			see Table II		*

TABLE IV. Values of $J_1(q)$ and $J_2(q)$ at points of high symmetries in the body-centered tetragonal lattice.

q	$J_1(q)$	$J_2(q)$
$\Gamma(0,0,0)$	$-V_0 + 2J_p$	$4J_c$
$M(\frac{1}{2}, \frac{1}{2}, 0)$	$-V_0 - 2J_p$	0
$X(\frac{1}{2}, 0, 0)$	$-V_0$	0
$Z(0, 0, \frac{1}{2})$	$-V_0 + 2J_p$	0
$A(\frac{1}{2}, \frac{1}{2}, \frac{1}{2})$	$-V_0 - 2J_p$	0
$R(\frac{1}{2}, 0, \frac{1}{2})$	$-V_0$	0

$$\frac{1}{N} \sum_q (\rho_{1q}, \rho_{2q}) \begin{pmatrix} V_1(q) & V_2(q) \\ V_2(q) & V_1(q) \end{pmatrix} \begin{pmatrix} \rho_{1-q} \\ \rho_{2-q} \end{pmatrix}, \quad (2.22)$$

where

$$V_1(q) = \frac{1}{4} V_0 + V_p (\cos q_1 a + \cos q_2 a), \quad (2.23)$$

$$V_2(q) = 4V_c \cos \frac{1}{2} q_1 a \cos \frac{1}{2} q_2 a \cos \frac{1}{2} q_3 c, \quad (2.24)$$

and the couplings between the spin densities are

$$\frac{1}{N} \sum_q \sum_j (s_{1q}^j, s_{2q}^j) \begin{pmatrix} J_1(q) & J_2(q) \\ J_2(q) & J_1(q) \end{pmatrix} \begin{pmatrix} s_{1-q}^j \\ s_{2-q}^j \end{pmatrix}, \quad (2.25)$$

with

$$J_1(q) = -V_0 + J_p (\cos q_1 a + \cos q_2 a), \quad (2.26)$$

$$J_2(q) = 4J_c \cos \frac{1}{2} q_1 a \cos \frac{1}{2} q_2 a \cos \frac{1}{2} q_3 c. \quad (2.27)$$

Values of $J_1(q)$ and $J_2(q)$ at points of high symmetries are listed in Table IV. The spin structure in URu_2Si_2 is that spins in each plane are ordered ferromagnetically and their directions alternate along the c axis; the antiferromagnetic wave vector is $(0,0,1)$. From Table IV, it is seen that if $J_p < 0$ (ferromagnetic) and $J_c > 0$ (antiferromagnetic), then the fluctuations at Γ point with antiphase between planes, $s_{1q} - s_{2q}$, are dominant. Therefore a possible superconducting state in URu_2Si_2 is either a singlet one, Γ_1^+ , Γ_4^+ , or Γ_5^+ , with the coupling constant of $V_c - \frac{3}{4}J_c$, or a triplet one, Γ_5^- , with the coupling constant of $V_p + \frac{1}{4}J_p$.

C. Hexagonal close-packed lattice

UPt_3 has a hexagonal Ni_3Sn structure (Fig. 2). The uranium sites form a hexagonal close-packed lattice, slightly modified from an ideal one along the c axis. Since there are two uranium atoms in the unit cell, we can use the same form as Eqs. (2.9)–(2.13) for the effective couplings. Of course the number of the nearest-neighbor sites and their directions (Fig. 2) are different from the bct lattice. For the ideal hcp lattice all nearest-neighbor sites in the plane and off the plane are equivalent. Therefore $V_p \cong V_c$ and $J_p \cong J_c$ for the ideal hcp lattice. On the other hand, J_p (V_p) can be quite different from J_c (V_c) in the bct lattice as we mentioned in Sec. II B.

Irreducible representations of the superconducting order parameter are listed in Table V for singlet pairings

TABLE V. Irreducible representations of singlet Cooper pairs in the hexagonal close-packed lattice with the nearest-neighbor couplings.

Γ	V_Γ	γ	$\phi^{11}(k)$	$\phi^{12}(k) = \phi^{21}(-k)$	$\phi^{22}(k)$
Γ_1^+	V_0		$\frac{1}{\sqrt{2}}$		$\frac{1}{\sqrt{2}}$
Γ_4^-	V_0		$\frac{1}{\sqrt{2}}$		*
Γ_1^+	$V_p - \frac{3}{4}J_p$		$\gamma_0(k)$		$\gamma_0(k)$
Γ_4^-	$V_p - \frac{3}{4}J_p$		$\gamma_0(k)$		*
Γ_5^+	$V_p - \frac{3}{4}J_p$	u	$\gamma_u(k)$		$\gamma_u(k)$
		v	$\gamma_v(k)$		$\gamma_v(k)$
Γ_6^-	$V_p - \frac{3}{4}J_p$	u	$\gamma_u(k)$		*
		v	$\gamma_v(k)$		*
Γ_1^+	$V_c - \frac{3}{4}J_c$			$\gamma_{c0}(k)$	$\frac{1}{\sqrt{3}} \cos \frac{1}{2} \mathbf{k} \cdot \mathbf{c} \left \sum_i e^{i\mathbf{k} \cdot \mathbf{d}_i} \right $
Γ_4^-	$V_c - \frac{3}{4}J_c$			$\gamma_{s0}(k)$	*
Γ_5^+	$V_c - \frac{3}{4}J_c$	u		$\gamma_{cu}(k)$	$\frac{\cos \frac{1}{2} \mathbf{k} \cdot \mathbf{c}}{\left \sum_i e^{i\mathbf{k} \cdot \mathbf{d}_i} \right } \gamma_u(k)$
		v		$\gamma_{cv}(k)$	$\frac{\cos \frac{1}{2} \mathbf{k} \cdot \mathbf{c}}{\left \sum_i e^{i\mathbf{k} \cdot \mathbf{d}_i} \right } \gamma_v(k)$
Γ_6^+	$V_c - \frac{3}{4}J_c$	u		$\gamma_{su}(k)$	$\frac{\sqrt{3} \sin \frac{1}{2} \mathbf{k} \cdot \mathbf{c}}{\left \sum_i e^{i\mathbf{k} \cdot \mathbf{d}_i} \right } \gamma_v(k)$
		v		$\gamma_{sv}(k)$	$\frac{\sqrt{3} \sin \frac{1}{2} \mathbf{k} \cdot \mathbf{c}}{\left \sum_i e^{i\mathbf{k} \cdot \mathbf{d}_i} \right } \gamma_u(k)$

and in Table VI for triplet pairings. An important difference from the bct lattice is that $\phi^{12}(k)$ is in general complex in the hcp lattice while it is real in the bct lattice. The reason is that the space group of the hcp lattice is not symmorphic. The point group of the hcp lattice is D_{6h} , but each atomic site does not have this symmetry, especially if it is not a center of inversion, hence complex $\phi^{12}(k)$. Another difference of the hcp lattice from the sc or the bct one is that it is not a bipartite lattice. There-

fore there is no simple rule for the transformation property of the basis functions under the shift of $\mathbf{k} \rightarrow \mathbf{k} + \mathbf{Q}$ except for the trivial case of the conventional s -wave superconductivity due to the on-site pairings.

Now we diagonalize the single-particle Hamiltonian, which has the form of Eq. (2.19). Again due to the non-symmorphic nature, $\epsilon_1(k)$ is not real in general. A typical example may be a single-particle Hamiltonian of the nearest-neighbor hoppings. In this case

TABLE VI. Irreducible representations of triplet Cooper pairs in the hexagonal close-packed lattice with the nearest-neighbor couplings.

Γ	V_Γ	γ	$\phi^{11}(k)$	$\phi^{12}(k) = -\phi^{21}(-k)$	$\phi^{22}(k)$
Γ_3^-	$V_p + \frac{1}{4}J_p$		$\gamma_o(k)$		$\gamma_o(k)$
Γ_4^-	$V_p + \frac{1}{4}J_p$		$\gamma_o(k)$		$-\gamma_o(k)$
Γ_6^-	$V_p + \frac{1}{4}J_p$	u'	$\gamma_u(k)$		$\gamma_u(k)$
		v'	$\gamma_v(k)$		$\gamma_v(k)$
Γ_5^+	$V_p + \frac{1}{4}J_p$	u'	$\gamma_u(k)$		$-\gamma_u(k)$
		v'	$\gamma_v(k)$		$-\gamma_v(k)$
Γ_4^-	$V_c + \frac{1}{4}J_c$			$\gamma_{c0}(k)$	*
$\Gamma_1^- 1$	$V_c + \frac{1}{4}J_c$			$\gamma_{s0}(k)$	$\frac{1}{\sqrt{3}} \sin \frac{1}{2} \mathbf{k} \cdot \mathbf{c} \left \sum_i e^{i\mathbf{k} \cdot \mathbf{d}_i} \right $
Γ_6^-	$V_c + \frac{1}{4}J_c$	u		$\gamma_{cu}(k)$	$\frac{\sqrt{3} \cos \frac{1}{2} \mathbf{k} \cdot \mathbf{c}}{\left \sum_i e^{i\mathbf{k} \cdot \mathbf{d}_i} \right } \gamma_v(k)$
		v		$\gamma_{cv}(k)$	$\frac{\sqrt{3} \cos \frac{1}{2} \mathbf{k} \cdot \mathbf{c}}{\left \sum_i e^{i\mathbf{k} \cdot \mathbf{d}_i} \right } \gamma_u(k)$
Γ_5^-	$V_c + \frac{1}{4}J_c$	u		$\gamma_{su}(k)$	$\frac{\sin \frac{1}{2} \mathbf{k} \cdot \mathbf{c}}{\left \sum_i e^{i\mathbf{k} \cdot \mathbf{d}_i} \right } \gamma_u(k)$
		v		$\gamma_{sv}(k)$	$\frac{\sin \frac{1}{2} \mathbf{k} \cdot \mathbf{c}}{\left \sum_i e^{i\mathbf{k} \cdot \mathbf{d}_i} \right } \gamma_v(k)$

$$\gamma_o(k) = \frac{1}{\sqrt{3}} (\cos \mathbf{k} \cdot \boldsymbol{\delta}_1 + \cos \mathbf{k} \cdot \boldsymbol{\delta}_2 + \cos \mathbf{k} \cdot \boldsymbol{\delta}_3)$$

$$\gamma_u(k) = \left[\frac{2}{3} \right]^{1/2} [\cos \mathbf{k} \cdot \boldsymbol{\delta}_1 - \frac{1}{2} (\cos \mathbf{k} \cdot \boldsymbol{\delta}_2 + \cos \mathbf{k} \cdot \boldsymbol{\delta}_3)]$$

$$\gamma_v(k) = \frac{1}{\sqrt{2}} (\cos \mathbf{k} \cdot \boldsymbol{\delta}_2 - \cos \mathbf{k} \cdot \boldsymbol{\delta}_3)$$

$$\gamma_{c0}(k) = \frac{1}{\sqrt{3}} \cos \frac{1}{2} \mathbf{k} \cdot \mathbf{c} (e^{-i\mathbf{k} \cdot \mathbf{d}_1} + e^{-i\mathbf{k} \cdot \mathbf{d}_2} + e^{-i\mathbf{k} \cdot \mathbf{d}_3})$$

$$\gamma_{s0}(k) = \frac{1}{\sqrt{3}} \sin \frac{1}{2} \mathbf{k} \cdot \mathbf{c} (e^{-i\mathbf{k} \cdot \mathbf{d}_1} + e^{-i\mathbf{k} \cdot \mathbf{d}_2} + e^{-i\mathbf{k} \cdot \mathbf{d}_3})$$

$$\gamma_{cu}(k) = \left[\frac{2}{3} \right]^{1/2} \cos \frac{1}{2} \mathbf{k} \cdot \mathbf{c} [e^{-i\mathbf{k} \cdot \mathbf{d}_1} - \frac{1}{2} (e^{-i\mathbf{k} \cdot \mathbf{d}_2} + e^{-i\mathbf{k} \cdot \mathbf{d}_3})]$$

$$\gamma_{cv}(k) = \frac{1}{\sqrt{2}} \cos \frac{1}{2} \mathbf{k} \cdot \mathbf{c} (e^{-i\mathbf{k} \cdot \mathbf{d}_2} - e^{-i\mathbf{k} \cdot \mathbf{d}_3})$$

$$\gamma_{su}(k) = \left[\frac{2}{3} \right]^{1/2} \sin \frac{1}{2} \mathbf{k} \cdot \mathbf{c} [e^{-i\mathbf{k} \cdot \mathbf{d}_1} - \frac{1}{2} (e^{-i\mathbf{k} \cdot \mathbf{d}_2} + e^{-i\mathbf{k} \cdot \mathbf{d}_3})]$$

$$\gamma_{sv}(k) = \frac{1}{\sqrt{2}} \sin \frac{1}{2} \mathbf{k} \cdot \mathbf{c} (e^{-i\mathbf{k} \cdot \mathbf{d}_2} - e^{-i\mathbf{k} \cdot \mathbf{d}_3})$$

$$\gamma_o(k) = \frac{1}{\sqrt{3}} (\sin \mathbf{k} \cdot \boldsymbol{\delta}_1 + \sin \mathbf{k} \cdot \boldsymbol{\delta}_2 + \sin \mathbf{k} \cdot \boldsymbol{\delta}_3)$$

$$\gamma_u(k) = \left[\frac{2}{3} \right]^{1/2} [\sin \mathbf{k} \cdot \boldsymbol{\delta}_1 - \frac{1}{2} (\sin \mathbf{k} \cdot \boldsymbol{\delta}_2 + \sin \mathbf{k} \cdot \boldsymbol{\delta}_3)]$$

$$\gamma_v(k) = \frac{1}{\sqrt{2}} (\sin \mathbf{k} \cdot \boldsymbol{\delta}_2 - \sin \mathbf{k} \cdot \boldsymbol{\delta}_3)$$

$$\epsilon_0(k) = 2t_p \sum_i \cos \mathbf{k} \cdot \delta_i, \quad (2.28)$$

$$\epsilon_1(k) = 2t_c \cos \frac{1}{2} \mathbf{k} \cdot \mathbf{c} \sum_i e^{i\mathbf{k} \cdot \delta_i}, \quad (2.29)$$

where t_p , and t_c are the hopping matrix elements and δ_i ($i=1,2,3$) are the vectors connecting nearest-neighbor pairs in the plane,

$$\delta_1 = a(1,0,0), \quad \delta_2 = a \left[-\frac{1}{2}, \frac{\sqrt{3}}{2}, 0 \right],$$

$$\delta_3 = a \left[-\frac{1}{2}, -\frac{\sqrt{3}}{2}, 0 \right],$$

and $\pm \frac{1}{2} \mathbf{c} + \mathbf{d}_i$ ($i=1,2,3$) are the vectors connecting nearest-neighbor pairs between planes,

$$\mathbf{d}_1 = \frac{1}{3}(\delta_2 - \delta_3), \quad \mathbf{d}_2 = \frac{1}{3}(\delta_3 - \delta_1),$$

$$\mathbf{d}_3 = \frac{1}{3}(\delta_1 - \delta_2).$$

The unitary transformation to diagonalize the single-particle Hamiltonian is

$$\begin{pmatrix} c_{1k\alpha} \\ c_{2k\alpha} \end{pmatrix} = \frac{1}{\sqrt{2}} \begin{pmatrix} 1 & e^{i\theta_k} \\ -e^{-i\theta_k} & 1 \end{pmatrix} \begin{pmatrix} a_{1k\alpha} \\ a_{2k\alpha} \end{pmatrix}, \quad (2.30)$$

where θ_k is the phase of $\epsilon_1(k)$:

$$e^{i\theta_k} = \epsilon_1(k) / |\epsilon_1(k)|.$$

$c_{1k\alpha}$ and $c_{2k\alpha}$ are the annihilation operators for the upper, $\epsilon_0(k) + |\epsilon_1(k)|$, and lower, $\epsilon_0(k) - |\epsilon_1(k)|$, hybridized bands. In the last columns of the Tables V and VI we marked by * those irreducible representations which vanish when we take into account only pairings within the same hybridized bands, which is again a reasonable approximation.

Special care must be taken for those irreducible representations (the last six in Tables V and VI) which have their amplitudes between the planes. The basis functions of these irreducible representations in the new one particle basis set, $c_{1k\alpha}$ and $c_{2k\alpha}$, are

$$\pm \frac{1}{2} [\phi^{12}(k) e^{i\theta_{-k}} + \phi^{21}(k) e^{i\theta_k}]. \quad (2.31)$$

(+ for the upper band and - for the lower band). In the last columns shown are the basis functions for the upper band with the use of the phase given by the nearest-neighbor hoppings, Eq. (2.29). The phase has the transformation property $\theta_{-k} = -\theta_k$ under the inversion. By combining this transformation property with Eqs. (2.16) or Eq. (2.17), eventually the singlets have even parity and the triplets have odd parity. This is an important difference compared with a lattice of a symmmorphic space group, of which the bct lattice is an example.²⁵

Now we transform the effective couplings into expression in reciprocal space. The couplings between charge densities have the same form as Eq. (2.22), with

$$V_1(q) = \frac{1}{4} V_0 + V_p \sum_i \cos \mathbf{q} \cdot \delta_i, \quad (2.32)$$

TABLE VII. Values of $J_1(q)$ and $J_2(q)$ at points of high symmetries in the hexagonal close-packed lattice.

q	$J_1(q)$	$J_2(q)$
$\Gamma(0,0,0)$	$-V_0 + 3J_p$	$3J_0$
$A(0,0,\frac{1}{2})$	$-V_0 + 3J_p$	0
$M(\frac{1}{2},0,0)$	$-V_0 - J_p$	$J_c e^{(i\pi/3)i}$
$L(\frac{1}{2},0,\frac{1}{2})$	$-V_0 - J_p$	0
$K(\frac{1}{3},\frac{1}{3},0)$	$-V_0 - \frac{3}{2}J_p$	0
$H(\frac{1}{3},\frac{1}{3},\frac{1}{2})$	$-V_0 - \frac{3}{2}J_p$	0

$$V_2(q) = V_c \cos \frac{1}{2} \mathbf{q} \cdot \mathbf{c} \sum_i e^{i\mathbf{q} \cdot \mathbf{d}_i}. \quad (2.33)$$

The couplings between the spin densities have also the same form as Eq. (2.25) with

$$J_1(q) = -V_0 + J_p \sum_i \cos \mathbf{q} \cdot \delta_i, \quad (2.34)$$

$$J_2(q) = J_c \cos \frac{1}{2} \mathbf{q} \cdot \mathbf{c} \sum_i e^{i\mathbf{q} \cdot \mathbf{d}_i}. \quad (2.35)$$

Values of $J_1(q)$ and $J_2(q)$ at points of high symmetries are listed in Table VII.

According to Aeppli *et al.*¹¹ the antiferromagnetic wave vector \mathbf{Q} is $(\frac{1}{2}, 0, 1)$ at the M point. It is seen from Table VII that eigenvalue of Eq. (2.25) is the largest at the M point, $-V_0 - J_p - J_c$ for $s_{1q} - s_{2q} e^{-i\pi/3}$ if the coupling constants J_p and J_c are antiferromagnetic and nearly the same, $J_p \cong J_c > 0$. As we have discussed we expect $J_p \cong J_c$ in UPt_3 since the structure is close to the ideal hcp lattice. The spin structure of $s_{1q} - s_{2q} e^{-i\pi/3}$ at the M point is nothing but the spin structure reported by the neutron scattering.¹¹ Therefore the antiferromagnetic fluctuations around the M point are expected to be dominant fluctuations responsible for the superconductivity

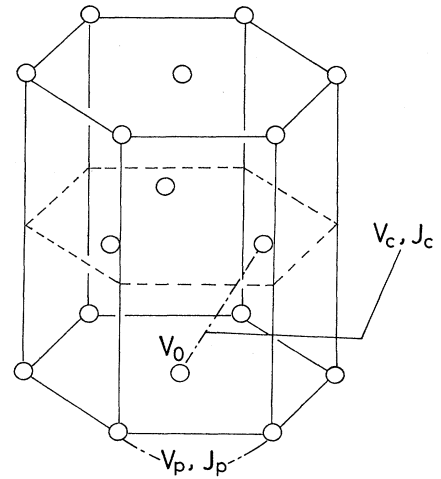


FIG. 2. Crystal structure of U atoms in UPt_3 . V_0 is the on-site coupling constant, V_p and V_c are the coupling constants between the nearest-neighbor charge densities, and J_p and J_c are the coupling constants between the nearest-neighbor spin densities.

in UPt₃.²⁶ In that case the most probable superconducting state may be a singlet one, Γ_1^+ or Γ_5^+ with the coupling constant $V_p - \frac{3}{4}J_p$, or Γ_1^+ , Γ_5^+ , or Γ_6^+ with $V_c - \frac{3}{4}J_c$. Since $V_p \cong V_c$ and $J_p \cong J_c$, if Γ_1^+ (or Γ_5^+) is realized, the order parameter may be a linear combination of the two Γ_1^+ (or Γ_5^+) representations.

III. COUPLING BETWEEN SUPERCONDUCTIVITY AND ANTIFERROMAGNETISM

In this section we derive the expression of the coupling term between superconductivity and antiferromagnetism. Heavy-electron materials which show the coexistence phenomena between superconductivity and antiferromagnetism have a characteristic feature; the magnitude of ordered moment is small, as we mentioned in Sec. I. For example, the ordered moment in URu₂Si₂ (Ref. 9) is $(0.03 \pm 0.01)\mu_B$ and that in UPt₃ is $(0.02 \pm 0.01)\mu_B$.¹¹ Because of that fact we may use Ginzburg-Landau expansion of the free energy not only by the superconducting order parameter but also by the antiferromagnetic order parameter.

An advantage of the Ginzburg-Landau-type theory is that the group theoretical argument can be used. Firstly, the general form of the coupling term between the superconducting order parameter and the antiferromagnetic one is obtained. Secondly, based on the general form the compatibility of each state classified in Sec. II is discussed. In the present scheme we need not assume a unitary state for the superconductivity, as usually done; a nonunitary state may be discussed on the same footing.

It is obvious that the lowest-order coupling between the superconductivity and the antiferromagnetism in the Ginzburg-Landau free energy is quadratic with respect to both order parameters. It is a consequence of the gauge invariance and the time-reversal symmetry. Therefore the coupling term is derived either by expanding the staggered susceptibility by the superconducting order parameter or by expanding the gap function by the staggered moment. We use the former method in this paper because it is more transparent and convenient to use the Green's-function method. Of course, the two methods given the same result.

In the calculation of the coupling term, we use a weak-coupling approximation. By the weak-coupling approximation, we mean that under the assumption the antiferromagnetic coupling constant does not depend on the superconducting order parameter. Equivalently in the second approach the weak-coupling approximation means that the superconducting coupling constant does not depend on the staggered moment. Strong coupling corrections are neglected in this section. However, it is easy to see the general form of the Ginzburg-Landau free energy including the strong-coupling corrections since the necessary symmetries have been taken into account already in the weak-coupling limit.

In the following we use the hcp case to illustrate detailed procedure of derivation. For the bct and the sc cases, we will show only final results.

A. Green's function

As a preliminary step to calculate the susceptibility we study the Green's functions in the presence of the superconducting order parameter.

1. Hexagonal close-packed lattice

We begin with the Hamiltonian for the hcp lattice. In the unit cell of the hcp lattice there are two atomic orbitals. We use two operators $c_{1k\alpha}$, and $c_{2k\alpha}$ defined by Eq. (2.30) which diagonalize the noninteracting Hamiltonian, Eq. (2.18). We assume that Cooper pairs are formed by electrons, $k\alpha$ and $-k\beta$, in the same band, because the energy of the $k\alpha$ state in one band is generally different from that of $k\beta$ state in the other band. On the other hand, if they are in the same band they have the same energy because of the inversion symmetry. The mean-field Hamiltonian is of the form

$$H = \sum_{k,m,s} \omega_m(k) c_{mks}^\dagger c_{mks} + \frac{1}{2} \sum_{k,m} \sum_{s_1,s_2} \sum_j d_j^m(k) c_{mks_1}^\dagger (i\sigma_j^\dagger \sigma_2)_{s_1 s_2} c_{m-k s_2} - \frac{1}{2} \sum_{k,m} \sum_{s_1,s_2} \sum_j d_j^{m*}(k) c_{m-k s_1} (i\sigma_2 \sigma_j)_{s_1 s_2} c_{mks_2} \quad (3.1)$$

with

$$\omega_1(k) = \epsilon_0(k) + |\epsilon_1(k)|, \quad (3.2)$$

$$\omega_2(k) = \epsilon_0(k) - |\epsilon_1(k)|,$$

where the suffix m denotes the upper hybridized band $\omega_1(k) = \epsilon_0(k) + |\epsilon_1(k)|$ for $m=1$, and the lower hybridized band $\omega_2(k) = \epsilon_0(k) - |\epsilon_1(k)|$ for $m=2$. An example of the explicit forms of $\epsilon_0(k)$ and $\epsilon_1(k)$ is given by the nearest-neighbor hopping model, Eqs. (2.28) and (2.29). For the gap matrix we use the same four-vector notation as Eq. (2.7). The superconducting order parameters $d_0^m(k)$, $d_j^m(k)$ ($j=1,2,3$) are defined as follows:

$$d_0^m(k) = \frac{1}{N} \sum_{\Gamma_s, \gamma_{\Gamma_s}} V_{\Gamma_s} \langle \psi_{\gamma_{\Gamma_s}}^{(0)} \rangle \phi_{\gamma_{\Gamma_s}}^m(k), \quad (3.3)$$

$$d_j^m(k) = \frac{1}{N} \sum_{\Gamma_t, \gamma_{\Gamma_t}} V_{\Gamma_t} \langle \psi_{\gamma_{\Gamma_t}}^{(j)} \rangle \phi_{\gamma_{\Gamma_t}}^m(k), \quad (3.4)$$

where the coupling constants V_Γ and the basis functions $\phi_{\gamma_\Gamma}^m(k) = \phi_{\gamma_\Gamma}^{mm}(k)$ are obtained in Sec. II.

The Green's functions are defined as usual:

$$G_{\alpha\beta}^m(k, \tau) = - \langle T_\tau [c_{mk\alpha}(\tau) c_{mk\beta}^\dagger] \rangle,$$

$$F_{\alpha\beta}^m(k, \tau) = - \langle T_\tau [c_{mk\alpha}(\tau) c_{m-k\beta}] \rangle, \quad (3.5)$$

$$F_{\alpha\beta}^{m\dagger}(k, \tau) = - \langle T_\tau [c_{m-k\alpha}^\dagger(\tau) c_{mk\beta}^\dagger] \rangle,$$

where $G_{\alpha\beta}^m(k, \tau)$ is the normal Green's function and $F_{\alpha\beta}^m(k, \tau)$, $F_{\alpha\beta}^{m\dagger}(k, \tau)$ are the anomalous Green's functions. Since we have taken into account only pairings within the same band, all Green's functions are diagonal in the band indices. The Dyson equations of the Green's functions are

$$[i\omega_n - \omega_m(k)]G_{\alpha\beta}^m(k, i\omega_n) - \sum_j \sum_{s_1} d_j^m(k)(i\sigma_j^\dagger \sigma_2)_{\alpha s_1} F_{s_1\beta}^{m\dagger}(k, i\omega_n) = \delta_{\alpha\beta}, \quad (3.6a)$$

$$[i\omega_n + \omega_m(k)]F_{\alpha\beta}^{m\dagger}(k, i\omega_n) + \sum_j \sum_{s_1} d_j^{m*}(k)(i\sigma_2 \sigma_j)_{\alpha s_1} G_{s_1\beta}^m(k, i\omega_n) = 0, \quad (3.6b)$$

$$[i\omega_n - \omega_m(k)]F_{\alpha\beta}^m(k, i\omega_n) + \sum_j \sum_{s_1} d_j^m(k)(i\sigma_j^\dagger \sigma_2)_{\alpha s_1} G_{\beta s_1}^m(-k, -i\omega_n) = 0. \quad (3.6c)$$

We need to calculate the susceptibility up to the second order of the superconducting order parameter. Since the anomalous Green's functions $F_{\alpha\beta}^m(k, i\omega_n)$ and $F_{\alpha\beta}^{m\dagger}(k, i\omega_n)$ always appear in pairs in the susceptibility, it is sufficient to replace $G_{\gamma\beta}^m(k, i\omega_n)$ by the free Green's function

$$G_{\alpha\beta}^{0m}(k, i\omega_n) = \frac{\delta_{\alpha\beta}}{i\omega_n - \omega_m(k)} \quad (3.7)$$

in Eqs. (3.6b) and (3.6c). The solution for the normal Green's function $G_{\alpha\beta}^m(k, i\omega_n)$ is obtained by substituting $F_{\alpha\beta}^{m\dagger}(k, i\omega_n)$ obtained in this manner. The results are

$$\begin{aligned} F_{\alpha\beta}^m(k, i\omega_n) &= -\frac{1}{\omega_m^2(k) + \omega_n^2} \sum_j d_j^m(k)(i\sigma_j^\dagger \sigma_2)_{\alpha\beta}, \\ F_{\alpha\beta}^{m\dagger}(k, i\omega_n) &= \frac{1}{\omega_m^2(k) + \omega_n^2} \sum_j d_j^{m*}(k)(i\sigma_2 \sigma_j)_{\alpha\beta}, \\ G_{\alpha\beta}^m(k, i\omega_n) &= \frac{\delta_{\alpha\beta}}{i\omega_n - \omega_m(k)} \\ &\quad + \frac{\sum_{jj'} d_j^m(k) d_{j'}^{m*}(k) (\sigma_j^\dagger \sigma_{j'})_{\alpha\beta}}{[i\omega_n - \omega_m(k)][\omega_m^2(k) + \omega_n^2]}. \end{aligned} \quad (3.8)$$

2. Body-centered tetragonal lattice

In the unit cell of the bct lattice, there are two atomic orbitals like the hcp lattice. We calculate the Green's functions under the same assumption as we used for the hcp lattice. The Green's functions for the bct lattice are of the same form as those for the hcp lattice, Eq. (3.8).

3. Simple cubic lattice

In the unit cell of the sc lattice there is one atomic orbital unlike the hcp lattice and the bct one. The Green's functions in the sc lattice are easily obtained by suppress-

ing the band indices in Eqs. (3.8). In numerical calculations in the Sec. III E we will use $\omega(k)$ of the tight binding model

$$\omega(k) = -t \sum_i \cos(\mathbf{k} \cdot \mathbf{a}_i), \quad (3.9)$$

where t is the hopping matrix element and \mathbf{a}_i ($i=1,2,3$) are the vectors connecting nearest-neighbor pairs.

B. Susceptibility

Now we proceed to susceptibility. We illustrate procedure of calculations of the staggered susceptibility using the hcp lattice as an example, as we did in Sec. III A.

1. Hexagonal close-packed lattice

As we discussed in the Sec. II C, the spin density fluctuations around $s_{1q} - s_{2q} e^{-i\pi/3}$ at the M point are the most enhanced. The corresponding staggered susceptibility $\chi_Q^{ll'}$ ($l, l' = x, y, z$) is defined as

$$\chi_Q^{ll'} = \int_0^\beta d\tau \langle S_Q^l(\tau) S_{-Q}^{l'}(0) \rangle, \quad (3.10)$$

where S_Q^l is the l component of the staggered magnetization. We rewrite the staggered magnetization S_Q^l with the operators $c_{1k\alpha}, c_{2k\alpha}$ defined in Eq. (2.30) which diagonalize the noninteracting Hamiltonian,

$$S_Q^l = \sum_k \sum_{\alpha, \beta m, m'} (\sigma^l)_{\alpha\beta} \tau_{k, k+Q}^{mm'} c_{mk}^\dagger + Q c_{m'k\beta}, \quad (3.11)$$

with

$$\begin{aligned} \tau_{k, k+Q}^{11} &= \frac{1}{2} (1 - e^{i(\theta_k + q - \theta_k)} e^{-(\pi/3)i}), \\ \tau_{k, k+Q}^{12} &= -\frac{1}{2} e^{i\theta_k} (1 + e^{i(\theta_k + Q - \theta_k)} e^{-(\pi/3)i}), \\ \tau_{k, k+Q}^{21} &= -\frac{1}{2} e^{-i\theta_k} e^{-(\pi/3)i} \\ &\quad \times (1 + e^{-i(\theta_k + Q - \theta_k)} e^{(\pi/3)i}), \\ \tau_{k, k+Q}^{22} &= \frac{1}{2} e^{-(\pi/3)i} (e^{i(\theta_k + Q - \theta_k)} e^{(\pi/3)i} - 1), \end{aligned} \quad (3.12)$$

where $\tau_{k, k+Q}^{mm'}$ denotes the matrix element of transition $(m, k) \rightarrow (m', k+Q)$. Since we want to calculate the free energy up to second order of the superconducting order parameter, we can use Eq. (3.7) for the Green's function. We substitute Eqs. (3.11) into Eq. (3.10) and the staggered susceptibility is expressed by the Green's functions:

$$\begin{aligned} \chi_Q^{ll'} &= T \sum_{i\omega_n} \sum_{\alpha, \beta \alpha', \beta'} \sum_k \sum_{m_1, m_2} |\tau_{k, k+Q}^{m_1 m_2}|^2 [-(\sigma^l)_{\alpha\beta} (\sigma^{l'})_{\alpha'\beta'} G_{\beta\alpha}^{m_1}(k+Q, i\omega_n) G_{\alpha\beta}^{m_2}(k, i\omega_n) \\ &\quad + (\sigma^l)_{\alpha\beta} (\sigma^{l'})_{\alpha'\beta'} F_{\alpha\alpha'}^{m_1\dagger}(k+Q, i\omega_n) F_{\beta\beta'}^{m_2}(k, i\omega_n)]. \end{aligned} \quad (3.13)$$

After the frequency summation Eq. (3.13) is rewritten as follows:

$$\chi_Q^{ll'} = \chi_{0Q}^{ll'} + \delta\chi_Q^{ll'}, \quad (3.14a)$$

$$\chi_{0Q}^{ll'} = -\text{Tr}(\sigma^l \sigma^{l'}) \sum_k \sum_{m_1, m_2} \frac{f[\omega_{m_1}(k+Q)] - f[\omega_{m_2}(k)]}{\omega_{m_1}(k+Q) - \omega_{m_2}(k)}, \quad (3.14b)$$

$$\begin{aligned} \delta\chi_Q^{ll'} = & \delta_{l,l'} \sum_{m_1, m_2} \sum_k [\gamma_1^{m_1 m_2}(k) + \gamma_2^{m_1 m_2}(k)] \sum_{j, j'} \text{Tr}[d_j^{m_2}(k) d_{j'}^{m_2*}(k) \sigma_j^\dagger \sigma_{j'}] \\ & + \sum_{m_1, m_2} \sum_k \gamma_2^{m_1 m_2}(k) \sum_{j, j'} \text{Tr}[d_j^{m_1*}(k+Q) d_{j'}^{m_2}(k) \sigma_j \sigma_l \sigma_{j'} \sigma_{l'}] \end{aligned} \quad (3.14c)$$

with

$$\gamma_1^{m_1 m_2}(k) = \frac{1}{2} \frac{|\tau_{k, k+Q}^{m_1 m_2}|^2}{\omega_{m_1}(k+Q) - \omega_{m_2}(k)} \frac{\partial}{\partial \omega_{m_2}(k)} \left[\frac{1}{\omega_{m_2}(k)} \tanh \frac{\beta \omega_{m_2}(k)}{2} \right], \quad (3.15)$$

$$\begin{aligned} \gamma_2^{m_1 m_2}(k) = & \frac{|\tau_{k, k+Q}^{m_1 m_2}|^2}{[\omega_{m_1}(k+Q) - \omega_{m_2}(k)]^2} \\ & \times \left[\frac{1}{\omega_{m_2}(k)} \tanh \frac{\beta \omega_{m_2}(k)}{2} - \frac{1}{\omega_{m_2}(k) + \omega_{m_1}(k+Q)} \left[\tanh \frac{\beta \omega_{m_2}(k)}{2} + \tanh \frac{\beta \omega_{m_1}(k+Q)}{2} \right] \right], \end{aligned}$$

where $\chi_{0Q}^{ll'}$ is the staggered susceptibility without the superconducting order parameter and $\delta\chi_Q^{ll'}$ is the deviation from it. In the above expression $f(x)$ is the Fermi distribution function and the fact that $\mathbf{k} + \mathbf{Q}$ is equivalent to $\mathbf{k} - \mathbf{Q}$ has been used.

2. Body-centered tetragonal lattice

The staggered susceptibility for the bct lattice has the same expression for the hcp lattice, Eq. (3.14). The only difference is the expressions of $\tau_{k, k+Q}^{m_1 m_2}$,

$$\begin{aligned} \tau_{k, k+Q}^{11} &= \frac{1}{2} [1 - \text{sgn} \epsilon_1(k+Q) \text{sgn} \epsilon_1(k)], \\ \tau_{k, k+Q}^{12} &= -\frac{1}{2} [\text{sgn} \epsilon_1(k) + \text{sgn} \epsilon_1(k+Q)], \\ \tau_{k, k+Q}^{21} &= \tau_{k, k+Q}^{12}, \quad \tau_{k, k+Q}^{22} = -\tau_{k, k+Q}^{11}. \end{aligned} \quad (3.16)$$

$$\gamma_1(k) = \frac{1}{2} \frac{1}{\omega(k+Q) - \omega(k)} \frac{\partial}{\partial \omega(k)} \left[\frac{1}{\omega(k)} \tanh \frac{\beta \omega(k)}{2} \right],$$

$$\gamma_2(k) = \frac{1}{[\omega(k+Q) - \omega(k)]^2} \left[\frac{1}{\omega(k)} \tanh \frac{\beta \omega(k)}{2} - \frac{1}{\omega(k) + \omega(k+Q)} \left[\tanh \frac{\beta \omega(k)}{2} + \tanh \frac{\beta \omega(k+Q)}{2} \right] \right]. \quad (3.18)$$

C. Free energy

Now we are at the position where we can calculate the coupling term between the superconductivity and antiferromagnetism in the free energy. The magnetic part of the free energy $F_M^{(2)}$ is

$$F_M^{(2)} = \frac{1}{2} \sum_{l, l'} M_Q^l [(\chi_Q^{-1})^{ll'} - I \delta_{l, l'}] M_Q^{l'}, \quad (3.19)$$

where M_Q^l is the staggered magnetization, $\chi_Q^{ll'}$ is the staggered susceptibility, and I is the interaction constant responsible for the antiferromagnetism. The coupling term is obtained by expanding the susceptibility as

$$[(\chi_Q^{-1})^{ll'}]^{ll'} = -\frac{\delta\chi_Q^{ll'}}{\chi_Q^{ll'} \chi_Q^{l'l}}, \quad (3.20)$$

3. Simple-cubic lattice

As we mentioned in Sec. III A3, the results for the sc lattice are again obtained by suppressing the band indices in Eqs. (3.14) and (3.15). For later use, we write them explicitly:

$$\begin{aligned} \delta\chi_Q^{ll'} = & \delta_{l,l'} \sum_k [\gamma_1(k) + \gamma_2(k)] \sum_{j, j'} \text{Tr}[d_j(k) d_{j'}^*(k) \sigma_j^\dagger \sigma_{j'}] \\ & + \sum_k \gamma_2(k) \sum_{j, j'} \text{Tr}[d_j^*(k+Q) d_{j'}(k) \sigma_j \sigma_l \sigma_{j'} \sigma_{l'}], \end{aligned} \quad (3.17)$$

where $\delta\chi_Q^{ll'}$ is the change of the susceptibility due to the superconducting order parameter which we have calculated in Sec. III B. By defining the staggered magnetic field through

$$M_Q^l = \chi_Q^{ll'} B_Q^l, \quad (3.21)$$

the coupling term is of the form

$$F_{\Delta M} = -\frac{1}{2} \sum_{l, l'} B_Q^l \delta\chi_Q^{ll'} B_Q^{l'}. \quad (3.22)$$

1. Hexagonal close-packed lattice

By substituting Eq. (3.14c) into Eq. (3.22), we obtain the expression of the coupling term

$$\begin{aligned}
F_{\Delta M} = & \sum_{m_1, m_2} (\gamma_1^{m_1 m_2} + \gamma_2^{m_1 m_2}) \langle d_0^{m_2}(k) d_0^{m_2*}(k) + \mathbf{d}^{m_2}(k) \mathbf{d}^{m_2*}(k) \rangle \mathbf{B}_Q \cdot \mathbf{B}_Q \\
& + \sum_{m_1, m_2} \bar{\gamma}_2^{m_1 m_2} \langle d_0^{m_2}(k) d_0^{m_1*}(k+Q) \rangle \mathbf{B}_Q \cdot \mathbf{B}_Q \\
& + \sum_{m_1, m_2} \bar{\gamma}_2^{m_1 m_2} \langle [\mathbf{d}^{m_2}(k) \cdot \mathbf{B}_Q] [\mathbf{d}^{m_1*}(k+Q) \cdot \mathbf{B}_Q] \\
& \quad - [\mathbf{d}^{m_2}(k) \times \mathbf{B}_Q] [\mathbf{d}^{m_1*}(k+Q) \times \mathbf{B}_Q] \rangle
\end{aligned} \tag{3.23}$$

where $\langle \rangle$ denotes the average on the Fermi surface. In Eq. (3.23) the coefficients are defined as $\gamma_i^{m_1, m_2} = \sum_k \gamma_i^{m_1, m_2}(k)$ with energy cutoff for $\omega_m(k)$. $\bar{\gamma}_i^{m_1, m_2}$ is also given by the same k summation with additional energy cutoff for $\omega_m(k+Q)$. From Eq (3.23) we see that the coupling term is rotationally invariant in the spin space for the present model without the spin-orbit interaction.

2. Body-centered tetragonal lattice

The coupling term in the free energy for the bct lattice is given by precisely the same form as that for the hcp one.

3. Simple-cubic lattice

The coupling term in the free energy for the sc lattice is obtained by suppressing the band indices in Eq. (3.23) as we already mentioned.

D. Discussion of the coupling term

In this section we evaluate the total coupling constant for each representation obtained in Sec. II. The results will show relative trend for each representation to have the coexistence between the antiferromagnetism and the superconductivity. In this section we will begin discussions from the simplest case, i.e., the sc lattice.

1. Simple cubic lattice

The first line of the coupling term, Eq. (3.23) does not depend on specific irreducible representations. The second line, for singlet pairing, or the third one, for triplet pairing, depends on them. The difference comes from the behavior of $d_j(k)$ when k is shifted by the antiferromagnetic wave vector $\mathbf{Q}=(\pi, \pi, \pi)$.

For the second Γ_1^+ and Γ_3^+ , since $d_0(k+Q)=-d_0(k)$, the coupling term is proportional to $\gamma_1+\gamma_2-\bar{\gamma}_2$, while for the conventional singlet pairing, the first Γ_1^+ , it is pro-

portional to $\gamma_1+\gamma_2+\bar{\gamma}_2$. Therefore, for anisotropic singlet pairing, the coexistence is easier to occur than for the conventional one.

For the triplet pairing, Γ_4^- , the basis functions also change their sign, $\mathbf{d}(k+Q)=-\mathbf{d}(k)$. Therefore the coupling term has the lowest energy when $\mathbf{d}(k)$ is parallel to \mathbf{B}_Q independent of k . This is possible when there is no spin-orbit coupling, and the coupling term is proportional to $\gamma_1+\gamma_2-\bar{\gamma}_2$ just the same as the anisotropic singlet pairings. We summarize the results in Table VIII. For the triplet one, the spin-orbit coupling which is neglected in the table is important. With the spin-orbit coupling, it is impossible to make $\mathbf{d}(k)$ parallel to \mathbf{B}_Q independent of k , since at least two basis functions of the orbital part enter in the basis functions of the product representations, see Eq. (16) of Ref. 21. Therefore we expect the triplet state lies in the middle of the conventional singlet and the anisotropic singlets from the point of view of the coexistence.

2. Body-centered tetragonal lattice

In URu₂Si₂ the antiferromagnetic wave vector \mathbf{Q} is (0,0,1).⁹ We assume $\mathbf{Q}=(0,0,1)$ in the following analysis.

For singlet pairings which are based on the pairing between planes, $\Gamma_1^+(V_\Gamma=V_c-\frac{3}{4}J_c)$, $\Gamma_4^+(V_\Gamma=V_c-\frac{3}{4}J_c)$, and $\Gamma_5^+(V_\Gamma=V_c-\frac{3}{4}J_c)$, $d_0(k)$ changes its sign under the shift of $k \rightarrow k+Q$; $d_0(k+Q)=-d_0(k)$. The coupling term is

$$\begin{aligned}
& \sum_{m_1, m_2} [(\gamma_1^{m_1 m_2} + \gamma_2^{m_1 m_2}) \langle |d_0^{m_2}(k)|^2 \rangle \\
& \quad - \bar{\gamma}_2^{m_1 m_2} \langle d_0^{m_1*}(k) d_0^{m_2}(k) \rangle] \mathbf{B}_Q^2.
\end{aligned} \tag{3.24}$$

On the other hand, for pairings which are based on the pairings within planes, $\Gamma_1^+(V_\Gamma=V_0)$, $\Gamma_1^+(V_\Gamma=V_p-\frac{3}{4}J_p)$, and $\Gamma_3^+(V_\Gamma=V_p-\frac{3}{4}J_p)$, $d_0(k+Q)=d_0(k)$ and the coupling term is

$$\begin{aligned}
& \sum_{m_1, m_2} [(\gamma_1^{m_1 m_2} + \gamma_2^{m_1 m_2}) \langle |d_0^{m_2}(k)|^2 \rangle \\
& \quad + \bar{\gamma}_2^{m_1 m_2} \langle d_0^{m_1*}(k) d_0^{m_2}(k) \rangle] \mathbf{B}_Q^2.
\end{aligned} \tag{3.25}$$

Therefore, the coexistence is easier to occur in the case for those singlet pairings between planes, $\Gamma_1^+(V_\Gamma=V_c-\frac{3}{4}J_c)$, $\Gamma_4^+(V_\Gamma=V_c-\frac{3}{4}J_c)$, and $\Gamma_5^+(V_\Gamma=V_c-\frac{3}{4}J_c)$, than the pairings in the case within planes, $\Gamma_1^+(V_\Gamma=V_0)$, $\Gamma_1^+(V_\Gamma=V_p-\frac{3}{4}J_p)$, and $\Gamma_3^+(V_\Gamma=V_p-\frac{3}{4}J_p)$.

For the triplet pairings, $\Gamma_2^-(V_\Gamma=V_c+\frac{1}{4}J_c)$,

TABLE VIII. The coupling constants between the superconductivity and the antiferromagnetism in the simple cubic lattice.

Γ	V_Γ	Coupling constants
Γ_1^+	V_0	$\gamma_1+\gamma_2+\bar{\gamma}_2$
Γ_1^+	$V_1-\frac{3}{4}J_1$	$\gamma_1+\gamma_2-\bar{\gamma}_2$
Γ_3^+	$V_1-\frac{3}{4}J_1$	$\gamma_1+\gamma_2-\bar{\gamma}_2$
Γ_4^-	$V_1+\frac{1}{4}J_1$	$\gamma_1+\gamma_2-\bar{\gamma}_2$

$\Gamma_3^-(V_\Gamma = V_c + \frac{1}{4}J_c)$, and $\Gamma_5^-(V_\Gamma = V_c + \frac{1}{4}J_c)$, the basis functions also change their sign, $\mathbf{d}^m(k+Q) = -\mathbf{d}^m(k)$. Therefore, the coupling term has the lowest energy when $\mathbf{d}^{m_1}(k)$ and $\mathbf{d}^{m_2}(k)$ are parallel to \mathbf{B}_Q independent of k . This is possible when there is no spin-orbit coupling, as we discussed in the previous Sec. III D 1. For the triplet pairings, $\Gamma_5^-(V_\Gamma = V_p + \frac{1}{4}J_p)$, the basis function does not change its sign, $\mathbf{d}^m(k+Q) = \mathbf{d}^m(k)$. Therefore, the coupling term has the lowest energy when $\mathbf{d}^{m_1}(k)$ and $\mathbf{d}^{m_2}(k)$ are perpendicular to \mathbf{B}_Q and parallel each other independent of k . In the both cases the coupling term is

$$\sum_{m_1, m_2} [(\gamma_1^{m_1 m_2} + \gamma_2^{m_1 m_2}) \langle |\mathbf{d}^{m_2}(k)|^2 \rangle - \bar{\gamma}_2^{m_1 m_2} \langle \mathbf{d}^{m_1*}(k) \mathbf{d}^{m_2}(k) \rangle] B_Q^2. \quad (3.26)$$

With the spin-orbit coupling we expect the triplet state lies in the middle of the conventional singlet and the anisotropic singlets. The Q vector of (0,0,1) is expected for $J_p < 0$, and $J_c > 0$. Therefore either a singlet pairing between planes or a triplet pairing within planes is plausible from the point of view of the coupling constant V_Γ . The present results show that those singlet states are also favorable to the coexistence.

3. Hexagonal close-packed lattice

In UPt₃ the antiferromagnetic wave vector Q is reported as $(\frac{1}{2}, 0, 1)$ as we mentioned in Sec. II C.¹¹ In the following, $Q = (\frac{1}{2}, 0, 1)$ is assumed in necessary cases.

There is an important difference between the hcp case and the sc or the bct case. In the latter cases the coupling term gives different contribution of the free energy depending on irreducible representations as we discussed in Secs. III D 1 and III D 2, but it does not lift the degeneracy of each multidimensional irreducible representation. It is easily seen from the fact that $\langle \phi_\gamma(k) \phi_\gamma(k+Q) \rangle = 0$ for different basis functions in the same irreducible representation Γ because $\phi_\gamma(k+Q) = \pm \phi_\gamma(k)$. On the other hand in the hcp case the transformation property of $\phi_\gamma(k+Q)$ is not so simple. Here we use $\Gamma_5^+(V_\Gamma = V_p - \frac{3}{4}J_p)$ as an example. It is a two-dimensional representation and the basis functions $\gamma_u(k)$ and $\gamma_v(k)$ behave under the shift by Q

$$\gamma_u(k+Q) = -\frac{\sqrt{2}}{3}\gamma_0(k) - \frac{2}{3}\gamma_u(k) - \frac{1}{\sqrt{3}}\gamma_v(k), \quad (3.27a)$$

$$\gamma_v(k+Q) = \left[\frac{2}{3} \right]^{1/2} \gamma_0(k) - \frac{1}{\sqrt{3}}\gamma_u(k). \quad (3.27b)$$

Therefore the coupling term depends on a specific form of the linear combination of the two basis functions

$$d_0(k) = \cos(\theta)\gamma_u(k) + \sin(\theta)\gamma_v(k). \quad (3.28)$$

The angle θ is determined so that the free energy becomes the lowest. From Eqs. (3.23), (3.27a), and (3.27b) we obtain

$$\langle d_0(k) d_0^*(k+Q) \rangle = -\frac{2}{3} \left[\frac{1}{2} + \cos \left[\frac{\pi}{3} + 2\theta \right] \right]. \quad (3.29)$$

$\langle d_0(k) d_0^*(k+Q) \rangle$ is maximum and equal to $\frac{1}{3}$ when $\theta = \pi/3$. It is minimum and equal to -1 when $\theta = -\pi/6$. We have shown that the degeneracy in $\Gamma_5^+(V_\Gamma = V_p - \frac{3}{4}J_p)$ is removed by the coupling term. The degeneracies in the other multidimensional representations for the coupling term are removed in the same way. A general discussion that all the irreducible representations in the hcp lattice with the antiferromagnetic ordering are one dimensional is given by Ozaki and Machida based on group theoretical arguments.²³ The present theory has made it clear how it occurs.

E. Magnitude of coupling constants

We investigate the magnitude of coupling constants between the superconductivity and the antiferromagnetism in this section. We consider the simple cubic lattice (a bipartite lattice) with nearest-neighbor hoppings as an example. In that case since $\omega(k+Q) = -\omega(k)$ the coupling constants are given by

$$\gamma_1 = \frac{1}{4} \int_{-\omega_c}^{\omega_c} d\omega \rho(\omega + \mu) \frac{1}{\omega + \mu} \frac{\partial}{\partial \omega} \left[\frac{1}{\omega} \tanh \frac{\beta_c \omega}{2} \right], \quad (3.30)$$

$$\gamma_2 = \frac{1}{4} \int_{-\omega_c}^{\omega_c} d\omega \rho(\omega + \mu) \frac{1}{(\omega + \mu)^2} \times \left\{ \frac{1}{\omega} \tanh \frac{\beta_c \omega}{2} - \frac{1}{2\mu} \left[\tanh \left[\frac{\beta_c \omega}{2} + \beta_c \mu \right] - \tanh \frac{\beta_c \omega}{2} \right] \right\} \quad (3.31)$$

from Eq. (3.18). In the above expression β_c equals $1/k_B T_c$, μ is chemical potential, ρ is the density of states, and ω_c is a cutoff energy.

The coupling constants can be calculated analytically in the half-filled case

$$\gamma_1 = \gamma_2 = \frac{7}{32} \rho \zeta(3) \frac{1}{(\pi k_B T_c)^2} = \frac{1}{2} \rho b, \quad (3.32)$$

where b is the coefficient of the $|\Delta|^4$ term in the weak-coupling limit. This is very large. For the case of the half-filled band in a bipartite lattice, the Fermi surface nests perfectly, resulting in an insulating state below T_N . Therefore it is almost always impossible to have a superconducting state once the antiferromagnetism sets in.

Now we consider more general cases away from the half-filled band. Since the coupling term is obtained by expanding the staggered susceptibility, we expect that the order of magnitude of γ is in the range

$$\frac{1}{T_c^2} > \gamma > \frac{1}{(T_F^*)^2}, \quad (3.33)$$

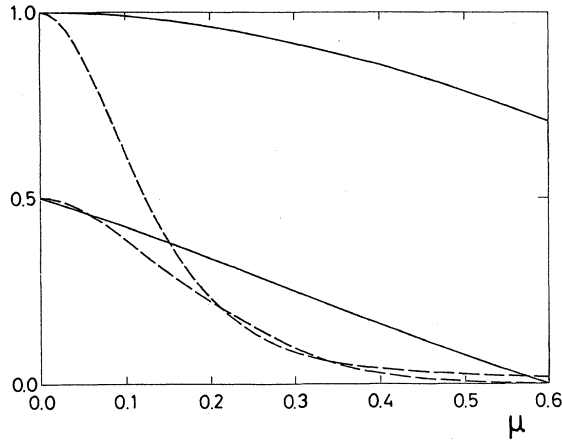


FIG. 3. Value of the coupling constant between the antiferromagnetism and the superconductivity $(\gamma_1 + \gamma_2)/2\gamma_1(\mu=0)$ and $\bar{\gamma}_2/2\gamma(\mu=0)$ as functions of chemical potential μ . The solid lines are for $T_c = D/10$. The dashed lines are for $T_c = D/100$. D is the bandwidth. In both cases the cutoff energy $\omega_c = D/10$.

where T_F^* is effective Fermi temperature. In heavy-electron systems, T_F^* is small, typically 10 or 20 K. Therefore we can expect sizable interference phenomena between the superconductivity and the antiferromagnetism in heavy-electron systems.

We show examples of numerical calculations in Fig. 3. We plot $(\gamma_1 + \gamma_2)/2\gamma_1(\mu=0)$ and $\bar{\gamma}_2/2\gamma_1(\mu=0)$ as functions of μ . In these examples we take $\omega_c = D/10$ where D is the bandwidth. The solid lines are for $T_c = D/10$. The dashed lines are for $T_c = D/100$. From Fig. 3 we see that the coupling constants are largest in the half-filled band and remain fairly large when the ratio of T_c to the bandwidth is relatively large, which may be a characteristic feature of the heavy-electron systems.

IV. ANALYSIS OF EXPERIMENTS

We have discussed the coupling term between the superconductivity and antiferromagnetism in Ginzburg-Landau free energy from a microscopic point of view in Sec. III. The coupling constant is determined from the band structure by Eqs. (3.15) and (3.18). In this section we take an alternative way. We analyze existing experimental data of URu_2Si_2 and UPt_3 and discuss the magnitude of the coupling constant.

A. Analysis of the Ginzburg-Landau free energy

Once we fix a particular superconducting state for a particular material, conventional or anisotropic one, we may write Ginzburg-Landau free energy as

$$F = \rho \left[-\frac{T_c^0 - T}{T_c^0} |\Delta|^2 + b |\Delta|^4 + \gamma |\Delta|^2 B_Q^2 - \frac{T_N - T}{T_N} \frac{1}{2} \delta B_Q^2 + \frac{1}{4} \delta \frac{B_Q^4}{B_0^2} \right] \quad (4.1)$$

by regarding Δ as the modulus of the order parameter.

In the above expression γ is the resultant coupling constant between the superconductivity and the antiferromagnetism, for example, $\gamma = \gamma_1 + \gamma_2 + \bar{\gamma}_2$ for the conventional superconductivity. We use the standard notation for the part of the free energy due to the superconductivity. T_c^0 is the superconducting transition temperature when $\gamma = 0$, ρ is the density of states, and b is the coefficient of the fourth-order term of Δ . In the weak-coupling theory $b = 7\zeta(3)/16(\pi k_B T_c)^2$. As for the part of the antiferromagnetism, T_N is the Néel temperature, B_0 is the staggered exchange field at $T = 0$ when $\gamma = 0$, and δ is a small constant of the order of unity.

The condition of the coexistence between the superconductivity and the antiferromagnetism is given by

$$\gamma B_0^2 < 1. \quad (4.2)$$

If this condition is satisfied the superconducting transition temperature is

$$T_c = \frac{1 - \gamma B_0^2}{1 - \gamma B_0^2 \frac{T_c^0}{T_N}} T_c^0 \quad (4.3)$$

and the exchange field below T_c is modified to

$$B_Q^2(T) = \frac{\left[1 - \frac{\gamma}{\delta b}\right] - \left[1 - \frac{\gamma}{\delta b} \frac{T_N}{T_c^0}\right] \frac{T}{T_N}}{1 - \frac{\gamma}{\delta b} \gamma B_0^2} B_0^2. \quad (4.4)$$

In the Ginzburg-Landau theory there is a jump of specific heat at T_N which is given by

$$\frac{1}{2} \rho \delta \left[\frac{B_0}{T_N} \right]^2. \quad (4.5)$$

B. Analysis of experimental data

1. URu_2Si_2

A big λ -type anomaly is observed in URu_2Si_2 . Equation Eq. (4.5) gives an estimate $\delta B_0^2 \cong T_N^2$. Then the coexistence condition, Eq. (4.2), can be expressed as $\gamma < \delta/T_N^2$. Since $T_N \cong T_F^*$, the coupling constant is relatively small in the range of Eq. (3.33). Using the weak-coupling expression for b we get $\gamma/b\delta < (T_c/T_N)^2$ from the inequality. From Eq. (4.4) we see that the present analysis predicts that there is no appreciable change in the temperature dependence of the $B_Q(T)$ or staggered magnetization $M_Q(T)$ at T_c ; in other words, $M_Q(T)$ continues to grow below T_c .

McElfresh *et al.*²⁷ measured pressure dependence of T_c and T_N . According to their results T_c vanishes at $P = 16$ Kbar, where $T_N = 20.5$ K. When we attribute the reduction of T_c solely to the coupling we get the upper limit of the coupling constant. It gives an estimation of $\gamma B_0^2 = \frac{7}{8}$. From the value, it follows that $T_c^0/T_N(P=0) = 0.43$. It shows that the value of the coupling constant is consistent with the original assumption that T_N is higher than T_c^0 .

2. UPt_3

The neutron experiments of UPt_3 reported that the staggered moment stopped to grow below T_c . From Eq. (4.4) the condition of this behavior is given by

$$\gamma = \delta \frac{T_c}{T_N} b \sim \frac{\delta}{T_c T_N}, \quad (4.6)$$

where the weak-coupling expression is used for b . It means the coupling constant γ is just at the middle of the range of Eq. (3.33). Then the coexistence condition can be expressed as $\delta B_0^2 < T_c T_N$. The first consequence of this result is that the jump of specific heat should be small, less than $T_c/T_N = 0.1$. The present analysis suggests a possible explanation for the absence of the specific heat anomaly at T_N in UPt_3 ; it is plausible that such a small anomaly may be smeared out by impurities.

The second point is that the coupling constant of the order of $\delta/T_c T_N$ is large. It is so large that in ordinary cases it is difficult to have the coexistence phenomena. The reason is that in ordinary cases we expect that the staggered exchange field is of order of T_N . Therefore it seems that the smallness of the ordered moment is necessary to have the coexistence in UPt_3 and the superconductivity is easily destroyed if the ordered moment becomes larger. In that sense it is interesting to note that in doped UPt_3 , $U(Pt_{1-x}Pd_x)_3$,¹ and $U_{1-x}Th_xPt_3$,²⁸ the ordered moment is bigger and the superconductivity is suppressed.

In summary, URu_2Si_2 has a small coupling constant and a large condensation energy due to the occurrence of the antiferromagnetism. On the other hand UPt_3 has a large coupling constant and a small condensation energy.

V. CONCLUSION

In the present paper we have investigated coexistence between the superconductivity and the antiferromagnetism from a general point of view. First we discuss classification of superconducting states in the simple cubic lattice as the simplest possible case, the body-centered tetragonal lattice relevant to URu_2Si_2 , and the hexagonal close-packed lattice relevant to UPt_3 . For that purpose we used the approach to describe the effective couplings for the superconductivity in real space. The advantage of the method is not only that the irreducible representations are determined unambiguously, but also that we can easily see the relation between the nature of fluctuations in the system and the superconducting states. In that way we discussed which states are favorable when the an-

tiferromagnetic fluctuations observed by the neutron scattering experiments are dominant mechanism for the superconductivity.

Secondly we obtained the coupling term between the superconductivity and the antiferromagnetism in the Ginzburg-Landau free energy. In this scheme we can obtain the general expression of the coupling constant in terms of the band structure. Here we would like to point out that in UPt_3 there is good agreement between band calculations^{29,30} and de Haas-van Alphen experiments, which is encouraging.³¹ The expression suggests that in heavy-fermion systems, where the effective Fermi temperature is small, we can expect considerable interference phenomena. We have also shown that many anisotropic superconducting states are more favorable to the coexistence than the conventional superconducting states. A typical example is the simple cubic lattice. In the example the extended s -wave states or the d wave state is the most favorable, the conventional s -wave state is the most unfavorable, and the p -wave states are in between.

The analysis of experimental data of UPt_3 and URu_2Si_2 was also done based on the Ginzburg-Landau theory. According to the analysis the coupling constant in UPt_3 is large. It is so large that the coexistence is only possible since the ordered moment or, more precisely, the staggered exchange field is so small. However, it seems that once the small ordered moment is accepted as fact the existing experimental data are mutually consistent including the smallness of the specific anomaly at T_N . On the other hand the coupling constant in URu_2Si_2 is relatively small and the coexistence here is an ordinary one. We would like to point out that the existence of such small ordered moment is a challenging problem to solid-state physicists.

ACKNOWLEDGMENTS

We are grateful to Toru Moriya for many helpful discussions. One of the authors (K.U.) would like to thank Maurice Rice and Frank Steglich for many discussions and their kind hospitality extended to him during his stay in Theoretische Physik, (ETHZ) Eidgenössische Technische Hochschule Zurich and Institute für Festkörperphysik, Technische Hochschule (TH), Darmstadt, where a part of the present work was done. The other author (R. K.) would like to thank Hisatoshi Yokoyama, Masao Ogata, Hirokazu Tsunetsugu, and Yoshinori Takahashi for helpful discussions. This work was supported by Grant-in-Aid for Scientific Research from the Ministry of Education, Science, and Culture.

¹For experiments see H. R. Ott, in *Progress in Low Temperature Physics*, edited by D. F. Brewer (North-Holland, Amsterdam, 1987), Vol. XI, Chap. 5, p. 215; U. Rauchschwalbe, *ibid.* *Physica B* **147**, 1 (1987); A. de Visser, A. Menovsky, and J. J. M. Franse, *ibid.* **147**, 81 (1987).

²For theories, see, for an example, P. A. Lee, T. M. Rice, J. W. Serene, L. J. Sham, and J. W. Wilkins, *Comments Cond. Mat. Phys.* **12**, 99 (1986).

³F. Steglich, J. Arts, C. D. Bredl, W. Lieke, D. Meschede, W.

Franz, and H. Schafer, *Phys. Rev. Lett.* **43**, 1892 (1979).

⁴H. R. Ott, H. Rudigier, Z. Fisk, and J. L. Smith, *Phys. Rev. Lett.* **50**, 1595 (1983).

⁵G. R. Stewart, Z. Fisk, J. O. Willis, and J. L. Smith, *Phys. Rev. Lett.* **52**, 679 (1984).

⁶W. Schlabitz, J. Baumann, B. Pollit, U. Rauchschwalbe, H. M. Mayer, U. Ahlheim, and C. D. Bredl, *Z. Phys. B* **62**, 171 (1986).

⁷T. T. M. Palstra, A. M. Menovsky, J. van den Berg, A. J. Dirk-

- maat, P. H. Kes, G. J. Nieuwenhuys, and J. A. Mydosh, *Phys. Rev. Lett.* **55**, 2727 (1985).
- ⁸M. B. Maple, J. W. Chen, Y. Dalichaouch, T. Kohara, C. Rossel, and M. S. Torikachvili, *Phys. Rev. Lett.* **56**, 185 (1986).
- ⁹C. Broholm, J. K. Kjems, W. J. L. Buyers, P. Matthews, T. T. M. Palstra, A. A. Menovsky, and J. A. Mydosh, *Phys. Rev. Lett.* **58**, 1467 (1987).
- ¹⁰D. W. Cook, R. H. Heffner, R. L. Huston, M. E. Schillaci, J. L. Smith, J. O. Willis, D. E. MacLaughlin, C. Boekema, R. L. Lichti, A. B. Denison, and J. Oostens, *Hyperfine Interact.* **31**, 425 (1986).
- ¹¹G. Aeppli, E. Bucher, C. Broholm, J. K. Kjems, J. Baumann, and J. Hufnagl, *Phys. Rev. Lett.* **60**, 615 (1988).
- ¹²Y. J. Uemura, W. J. Kossler, X. L. Yu, H. E. Schone, J. R. Kempton, C. E. Stronach, S. Barth, F. N. Gyax, B. Hitti, A. Schenok, C. Baines, W. F. Lankford, Y. Onuki, and T. Komatsubara (unpublished).
- ¹³H. Nakamura, Y. Kitaoka, H. Yamada, and K. Asayama (unpublished).
- ¹⁴K. Ueda and R. Konno (unpublished).
- ¹⁵H. R. Ott, H. Rudigier, T. M. Rice, K. Ueda, Z. Fisk, and J. L. Smith, *Phys. Rev. Lett.* **52**, 1915 (1984).
- ¹⁶P. W. Anderson, *Phys. Rev. B* **30**, 1549 (1984).
- ¹⁷F. J. Ohkawa and H. Fukuyama, *J. Phys. Soc. Jpn.* **53**, 4344 (1984).
- ¹⁸J. E. Hirsch, *Phys. Rev. Lett.* **54**, 1317 (1985).
- ¹⁹K. Miyake, S. Schmitt-Rink, and C. M. Varma, *Phys. Rev. B* **34**, 6554 (1986).
- ²⁰G. E. Volovik and L. P. Gor'kov, *Pis'ma Zh. Eksp. Teor. Fiz.* **39**, 550 (1984) [*JETP Lett.* **39**, 674 (1984)]; *Zh. Eksp. Teor. Fiz.* **88**, 1412 (1985) (*Sov. Phys.—JETP* **61**, 843 (1985)).
- ²¹K. Ueda and T. M. Rice, *Phys. Rev. B* **31**, 7114 (1985).
- ²²E. I. Blount, *Phys. Rev. B* **32**, 2935 (1985).
- ²³K. Kato, K. Machida, and M. Ozaki, *Jpn. Appl. Phys.* **26**, Suppl. **3**, 1245 (1987); M. Ozaki and K. Machida, *J. Phys. Soc. Jpn.* **57**, 398 (1988).
- ²⁴T. M. Rice and K. Ueda, *Phys. Rev. Lett.* **55**; 995 (1985); **55**, 2093(E) (1985).
- ²⁵The same type of classification of the hcp lattice is made by W. Putikka and R. Joynt, *Phys. Rev. B* **37**, 2372 (1988). However, they neglected the important role of the phase, but simply use $\frac{1}{2}[\phi^{12}(k) + \phi^{21}(k)]$ as the basis functions.
- ²⁶Another possibility may be the fluctuations around (0,0,1); M. Norman, *Phys. Rev. B* **37**, 4987 (1988).
- ²⁷M. W. McElfresh, J. D. Thompson, J. O. Willis, M. B. Maple, T. Kohara, and M. S. Torikachvili, *Phys. Rev. B* **35**, 43 (1987).
- ²⁸A. I. Goldman, G. Shirane, G. Aeppli, B. Batlogg, and E. Bucher, *Phys. Rev. B* **34**, 6564 (1986).
- ²⁹T. Oguchi, A. J. Freeman, and G. W. Crabtree, *Phys. Lett.* **117A**, 428 (1986).
- ³⁰C. S. Wang, M. R. Norman, R. C. Albers, A. M. Boring, W. E. Pickett, H. Krakauer, and N. E. Christensen, *Phys. Rev. B* **35**, 7260 (1987).
- ³¹L. Taillefer, R. Newbury, G. G. Lonzarich, Z. Fisk, and J. L. Smith, *J. Magn. Magn. Mater.* **63&64**, 372 (1987); L. Taillefer and G. G. Lonzarich, *Phys. Rev. Lett.* **60**, 1570 (1988).